

Imaging and Quantitation of Dopamine Transporters with Iodine-123-IPT in Normal and Parkinson's Disease Subjects

Hee-Joung Kim, Joo-Hyuk Im, Seoung-Oh Yang, Dae Hyuk Moon, Jin Sook Ryu, Jung-Kyun Bong, Ki-Pyo Nam, Jun-Hong Cheon, Myung-Chong Lee and Hee Kyung Lee

Departments of Nuclear Medicine and Neurology, Asan Medical Center, University of Ulsan, Seoul, Korea

Iodine-123-N-(3-iodopropene-2-yl)-2 β -carbomethoxy-3 β -(4-chlorophenyl) tropane (^{123}I -IPT) is a new dopamine transporter ligand that selectively binds the dopamine reuptake sites. Transporter concentrations have been known to decrease in Parkinson's disease patients. The purpose of this study was to evaluate the usefulness of IPT as an imaging agent for measuring changes in transporter concentrations in Parkinson's disease. **Methods:** IPT labeled with $6.78 \pm 0.67 \text{ mCi } ^{123}\text{I}$ was injected intravenously as a bolus into eight normal controls (mean age $41 \pm 12 \text{ yr}$) and 17 Parkinson's disease patients (mean age $55 \pm 9 \text{ yr}$). Dynamic SPECT scans of the brain were then performed for 5 min each over 120 min on a triple-headed gamma camera equipped with medium-energy collimators. Regions of interest were drawn on the middle set of the image at the level of the basal ganglia (BG) for each subject. Time-activity curves were generated for the left BG, right BG and occipital cortex (OCC). The empirical ratios between BG – OCC and OCC, which represent specific-to-nonspecific binding ratios, were computed at various time points. The statistical parameter k_3/k_4 was estimated by two methods: a variation of the graphic method that derives the ratio of ligand distribution volumes (R_V) and the area ratio method (R_A), in which the ratio is calculated from the areas under the specific and nonspecific binding activity curves. **Results:** The mean (BG – OCC)/OCC ratio for normal controls (3.07 ± 0.73) was significantly higher than that for Parkinson's disease patients at 115 min (1.10 ± 0.56) ($p = 2.76 \times 10^{-5}$). The mean R_V and R_A for normal controls were 2.06 ± 0.27 and 1.50 ± 0.15 , respectively. The mean R_V and R_A for Parkinson's disease patients were 0.78 ± 0.31 and 0.65 ± 0.24 , respectively. Both R_V and R_A for normal controls were significantly higher than those for Parkinson's disease patients (p values for R_V and R_A were 1.91×10^{-8} and 3.46×10^{-10} , respectively). The R_V has linear relationships with both R_A and (BG – OCC)/OCC ratio at 115 min. The R_V has a higher correlation ($r = 0.99$) with R_A than it does with (BG – OCC)/OCC ($r = 0.93$). **Conclusion:** The R_V , R_A and (BG – OCC)/OCC for Parkinson's disease patients were clearly separated from those of normal controls, and they may be useful outcome measures for clinical diagnosis. The simplest (BG – OCC)/OCC ratio, requiring a single late time point, could be useful in clinical situations, whereas R_V or R_A is preferred when the dynamic data are available. The findings suggest that ^{123}I -IPT is a useful tracer for diagnosing Parkinson's disease and studying dopamine reuptake sites.

Key Words: dopamine transporter; SPECT; Parkinson's disease

J Nucl Med 1997; 38:1703–1711

The dopamine transporter (i.e., reuptake site) serves to remove free dopamine from the synaptic cleft (1,2). Cocaine (3) and some of its tropane derivatives appear to be relatively specific for binding to dopamine reuptake sites (4), which play a central role in both the addictive properties of cocaine (3) and the

therapeutic actions of certain medications (5). Along with a recent advancement in PET and SPECT instrumentation and their processing techniques, several radiopharmaceuticals have been developed to image the dopamine transporters (6–13). In vivo PET and SPECT studies have shown that the dopamine transporter concentrations are decreased in Parkinson's patients (14,15) and increased in Tourette's syndrome (11).

The trans isomer of the N-iodopropenyl derivative, N-(3-iodopropene-2-yl)-2 β -carbomethoxy-3 β -(4-chlorophenyl) tropane (IPT) is a new promising ligand for the dopamine transporter with a binding affinity (K_d) of 0.2 nM in vitro (16,17). In vitro binding data using ^{125}I -IPT has suggested that binding is highly specific for the dopamine transporter. Preclinical studies in nonhuman primates have shown preferential uptake in the basal ganglia (BG) with a target to background contrast ratio of 22.8 at 3 hr postinjection (18). Dynamic SPECT scans in monkeys have shown that some indirectly acting dopaminergic drugs affect the uptake and elimination kinetics of IPT in the BG, whereas postsynaptic dopamine receptor antagonists do not. Displacement of the IPT uptake with monoamine transporters, mazindol, GBR-12909 and β -CIT (RTI-55) suggested that the binding is reversible (18). No pharmacological effects of the no-carrier-added tracer were observed in animal studies. Recently, Mozley et al. (19) have measured the radiation dosimetry of IPT in normal controls and have recommended injection of 7.5 mCi (280 MBq) of injection dose for the worst case in any organ and 13.5 mCi (500 MBq) for the critical organ by using the mean value. Ichise et al. (20) have developed a noninvasive method to estimate the receptor parameter k_3/k_4 in humans with iodine-123-iodobenzofuran (IBF)-SPECT.

Iodine-123- β -CIT has been widely used for SPECT dopamine transporter imaging (4,6,10,11), and its uptake in the BG peaked at 18–24 hr postinjection. This slow uptake may not be the optimal characteristics in clinical applications for SPECT dopamine transporter imaging studies. Iodine-123-IPT has shown much faster kinetics, and its uptake in the BG peaked at 1–2 hr postinjection.

We studied the usefulness of IPT as an imaging agent for measuring changes of transporter concentrations in Parkinson's disease. Transporter concentrations in normal controls and Parkinson's disease patients were estimated by three noninvasive methods: the empirical ratios between [BG – occipital cortex (OCC)] and OCC, which represent specific-to-nonspecific binding ratios at several time points, a variation of the graphic method that derives the ratio of ligand distribution volumes (R_V) (20,21) and the area ratio (R_A) method (22), in which the ratio is calculated from the areas under the specific and nonspecific binding activity curves. The modified graphic method developed by Ichise et al. (20) is assumed to be more

Received Sep. 27, 1996; revision accepted Feb. 28, 1997.

For correspondence or reprints contact: Hee-Joung Kim, PhD, Department of Diagnostic Radiology, Yonsei University, Medical College, 134 Shinchon-dong, Seodaemun-Ku, Seoul, Korea, 120-762.



TABLE 1
(BG – OCC)/OCC, R_A and R_V for Parkinson's Disease Patients

Subject no.	UPDRS	Stage by Hoehn and Yahr scale	(LBG – OCC)	(RBG – OCC)	(BG – OCC)	R _A , LBG	R _A , RBG	R _A	R _V , LBG	R _V , RBG	R _V
			OCC	OCC	OCC						
PP1	31	I	0.44	0.57	0.50	0.63	0.63	0.63	0.57	0.72	0.65
PP2	42	III	1.11	1.41	1.26	0.67	0.68	0.68	0.76	0.84	0.80
PP3	36	II	1.38	1.28	1.33	0.71	0.65	0.68	0.83	0.83	0.83
PP4	51	II	1.29	1.52	1.41	0.50	0.69	0.59	0.66	0.88	0.77
PP5	63	III	0.71	0.37	0.54	0.60	0.56	0.58	0.71	0.65	0.68
PP6	36	I	0.92	0.44	0.68	0.78	0.49	0.64	0.92	0.57	0.74
PP7	19	II	1.65	1.31	1.48	1.12	1.02	1.07	1.38	1.25	1.31
PP8	17	I	1.00	1.37	1.18	0.69	0.88	0.78	0.80	1.05	0.93
PP9	68	II	0.56	0.82	0.69	0.39	0.48	0.43	0.44	0.56	0.50
PP10	38	II	0.35	0.20	0.27	0.34	0.45	0.40	0.37	0.48	0.42
PP11	14	I	1.28	1.97	1.62	0.64	0.80	0.72	0.68	0.86	0.77
PP12	72	III	0.93	0.58	0.76	0.45	0.29	0.37	0.51	0.32	0.41
PP13	29	I	1.21	0.74	0.98	0.58	0.30	0.44	0.80	0.42	0.61
PP14	29	I	1.39	2.11	1.75	0.81	1.07	0.94	0.91	1.26	1.09
PP15	15	I	2.13	2.43	2.28	1.17	1.16	1.16	1.54	1.54	1.54
PP16	22	I	0.66	0.28	0.47	0.45	0.28	0.37	0.53	0.34	0.43
PP17	67	II	1.79	1.35	1.57	0.68	0.57	0.63	0.80	0.64	0.72
Mean			1.11	1.10	1.10	0.66	0.65	0.65	0.78	0.78	0.78
s.d.			0.47	0.65	0.56	0.22	0.26	0.24	0.29	0.33	0.31

L = left; R = right; PP = Parkinson's disease patient.

$$\frac{\int_0^t C_{BG}(t) dt}{C_{BG}(t)} = a \cdot \frac{\int_0^t fC_a(t) dt}{C_{BG}(t)} + b \quad \text{Eq. 1}$$

$$V = \frac{\int_0^\infty C_{BG}(t) dt}{\int_0^\infty fC_a(t) dt}, \quad \text{Eq. 4}$$

and

$$\frac{\int_0^t C_{OCC}(t) dt}{C_{OCC}(t)} = a' \cdot \frac{\int_0^t C_{BG}(t) dt}{C_{OCC}(t)} + b', \quad \text{Eq. 2}$$

for times in which the transport of ligand from plasma to tissue is unidirectional, where a , a' , b and b' are constants. Combination of Equations 1 and 2 after eliminating $fC_a(t)dt$ becomes (20):

$$\frac{\int_0^t C_{BG}(t) dt}{C_{BG}(t)} = \left(\frac{a}{a'}\right) \frac{\int_0^t C_{OCC} dt}{C_{BG}(t)} + \left(-\frac{ab'}{a'}\right) \frac{C_{OCC}(t)}{C_{BG}(t)} + b. \quad \text{Eq. 3}$$

Equation 3 is a multilinear equation with partial regression coefficients, a/a' , $-ab'/a'$ and b . These coefficients can be obtained by multiple regression analysis. The coefficient a/a' is related to equilibrium distribution volume, and R_V (V_3/V_2 or k_3/k_4) can be expressed $a/a' - 1$ (20). The coefficient a/a' was derived by multilinear regression analysis using built-in solver program in Microsoft Excel. The integrals in Equation 3 were obtained numerically by the trapezoid rule. R_V was obtained by subtracting 1 from a/a' .

Area Ratio Method

The regional equilibrium distribution volume of the IPT ligand, V , can be calculated by the following equations (22):

where $C_{BG}(t)$ represents BG activity. Two equations can be set up, one for the BG and the other for the OCC [where $C_{OCC}(t)$ represents OCC activity], which can be combined to yield one equation (20). Then, the ratio of the areas (R_A) under the specific binding and nondisplaceable activity curves can be expressed as (20,22):

$$R_A = \frac{\int_0^t C_{BG}(t) dt - \int_0^t C_{OCC}(t) dt}{\int_0^t C_{OCC}(t) dt} \rightarrow \frac{(V_3 + V_2) - V_2}{V_2^*} = \frac{V_3}{V_2} = \frac{k_3}{k_2} \text{ as } t \rightarrow \infty, \quad \text{Eq. 5}$$

R_A was measured using all 23 frames of data over 115 min, ignoring the data after 115 min. Ignoring time points after 115 min may cause an error in estimation of the total area under the curve (i.e., from 0 to infinity). Simple linear regression analysis was applied to check relationships among three outcome measures. Three outcome measures were used to see the difference between normal controls and Parkinson's disease patients. One-tailed Student's t -test was applied to obtain p values between normal control and Parkinson's disease patient for three outcome measures.

RESULTS

Labeling of Sn-IPT with Iodine-123

Iodine-123 produced using ^{124}Te target with no-carrier-added sodium was used for this study. The simplified labeling method

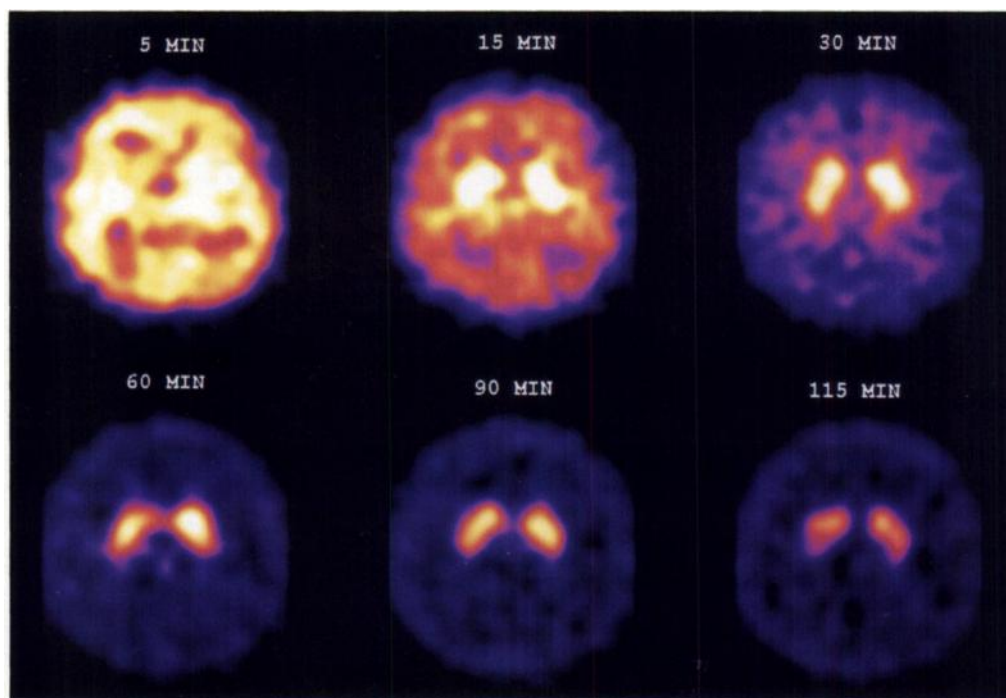


FIGURE 2. Activity distribution of ^{123}I -IPT after injection of 6.96 mCi (257.52 MBq) into a 49-yr-old female, normal control. Acquisitions were obtained for 5 min each with a triple-headed SPECT camera over 2 hr and reoriented so that the AC-PC line corresponded to the transaxial axis of the data set. Left BG-to-OCC ratios were 2.72, 4.15, 5.23 and 5.43 at 30, 60, 90 and 115 min, respectively. Right BG-to-OCC ratios were 2.54, 3.76, 5.11 and 5.16 at 30, 60, 90 and 115 min, respectively.

for the preparation of ^{123}I -IPT resulted in radiochemical yields of approximately 50%, with radiopharmaceutical purity of >90%.

Patients with Parkinson's Disease

All Parkinson's disease patients have idiopathic Parkinson's disease, which is now widely used to designate loss of presynaptic dopamine innervation. All Parkinson's disease patients except one had a convincing response to levodopa ($\geq 20\%$ change in UPDRS scores). One patient (PP7) could not receive levodopa due to development of peak dose dystonia of the neck after an initially good response for 1 wk. The results of UPDRS measurements are summarized in Table 1. Of the 17 Parkin-

son's disease patients, there were eight Hoehn and Yahr scale Stage I, six Stage II and three Stage III Parkinson's disease patients.

Dynamic SPECT Data

No subjective effects of ^{123}I -IPT tracer have been observed from normal controls and Parkinson's disease patients during the whole procedure, consisting of 2-hr dynamic scan periods. The radioactivities penetrate to the brain within 15 sec after injection, and BG activities in normal controls were visualized at late time points in the planar images. The BG activities in the reconstructed SPECT images peaked within 10 min postinjection for both normal controls and Parkinson's disease patients.

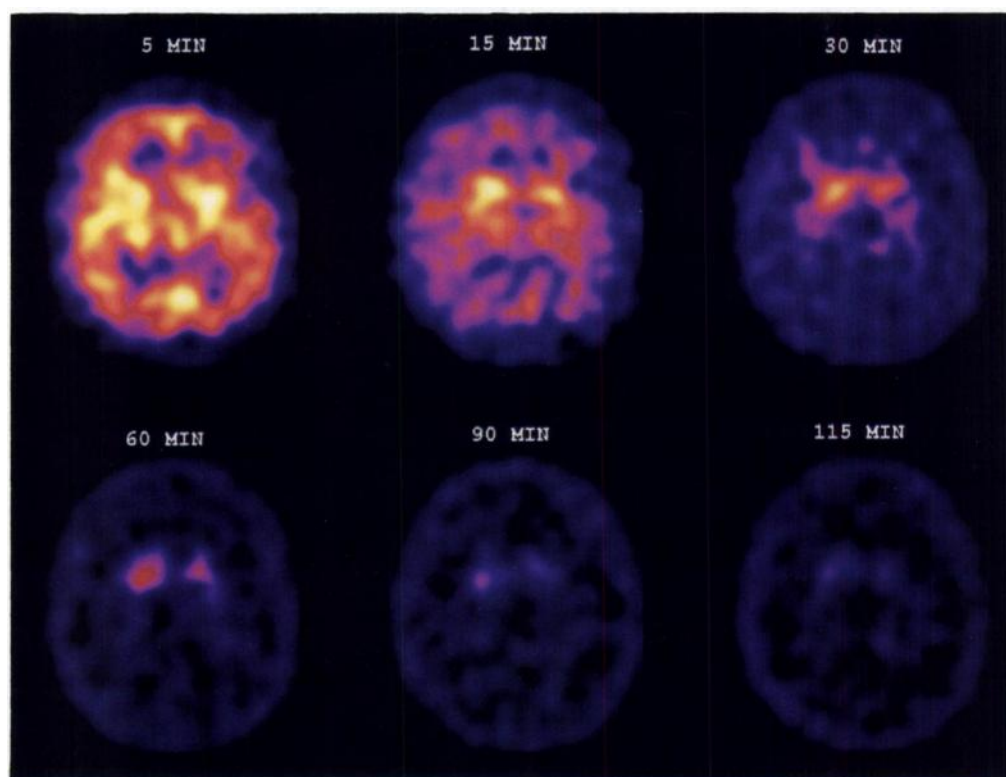


FIGURE 3. Activity distribution of ^{123}I -IPT after injection of 7.08 mCi (261.96 MBq) into a 49-yr-old man with early Parkinson's disease. Acquisitions were obtained for 5 min each with a triple-headed SPECT camera over 2 hr and reoriented so that the AC-PC line corresponded to the transaxial axis of the data set. Left BG-to-OCC ratios are 1.92, 2.85, 2.28 and 2.67 at 30, 60, 90 and 115 min, respectively. Right BG-to-OCC ratios were 2.27, 3.31, 2.53 and 3.46 at 30, 60, 90 and 115 min, respectively.

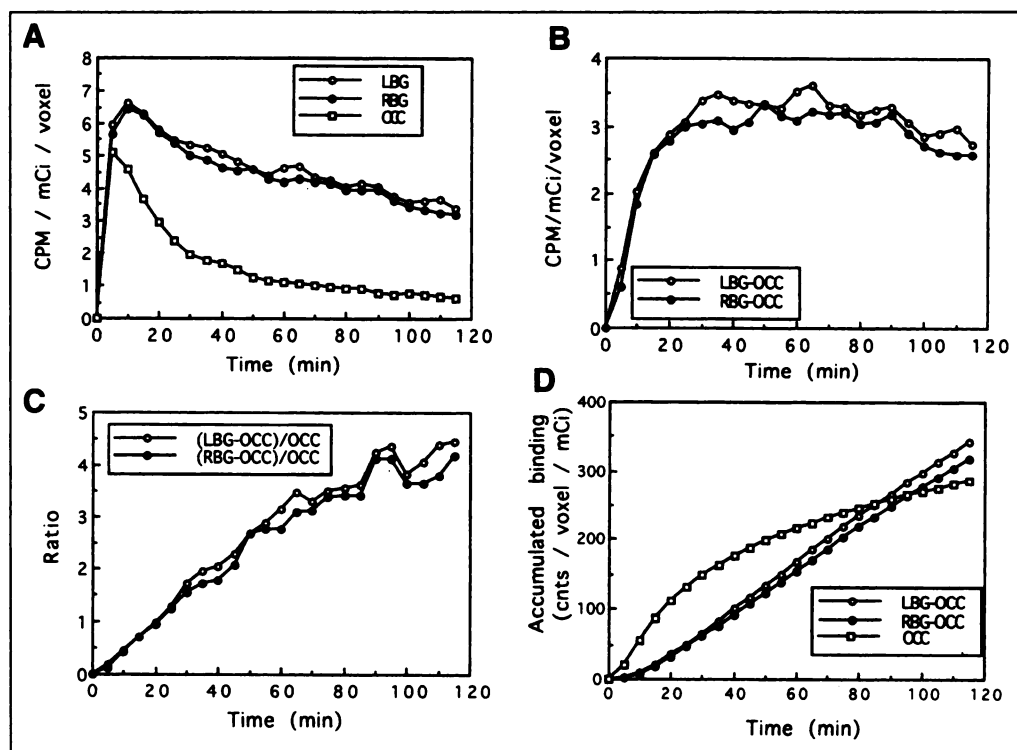


FIGURE 4. IPT time-activity curves for normal controls (Fig. 2). (A) Tissue curves. (B) Specific binding tissue curves. (C) Empirically defined specific binding ratio (BG - OCC)/OCC. (D) Accumulated specific binding curves.

The normal controls showed much slower washout kinetics than those for the Parkinson's disease patients (Figs. 2-5). The OCC, which was previously used as nonspecific site (32), peaked within 5 min postinjection for both normal controls and Parkinson's disease patients (Figs. 2-5). Unlike the BG, the OCC activities for both normal controls and Parkinson's disease patients showed very fast washout kinetics, indicating that the OCC may be nonspecific site and that there were few differences between normal controls and Parkinson's disease patients.

Simple Ratio Method

The simple ratio methods of specific-to-nonspecific binding activities [(BG - OCC)/OCC] have been used to measure

receptor parameters, with the assumption that late time point data may be sensitive to changes in receptor concentrations (11,18,33). The (BG - OCC)/OCC ratios for normal controls were continuously increased for 2 hr (Fig. 4C), whereas those for Parkinson's disease patients increased for 1 hr and became stable (Fig. 5C). The (BG - OCC)/OCC values for normal controls (3.07 ± 0.73) were significantly higher than those for Parkinson's disease patients (1.10 ± 0.56) at 115 min, and the *p* value was 2.76×10^{-5} (Fig. 6). However, the (BG - OCC)/OCC value between normal controls and Parkinson's disease patients was not clearly distinguished for 1 hr, indicating that the early time points may be more sensitive to changes

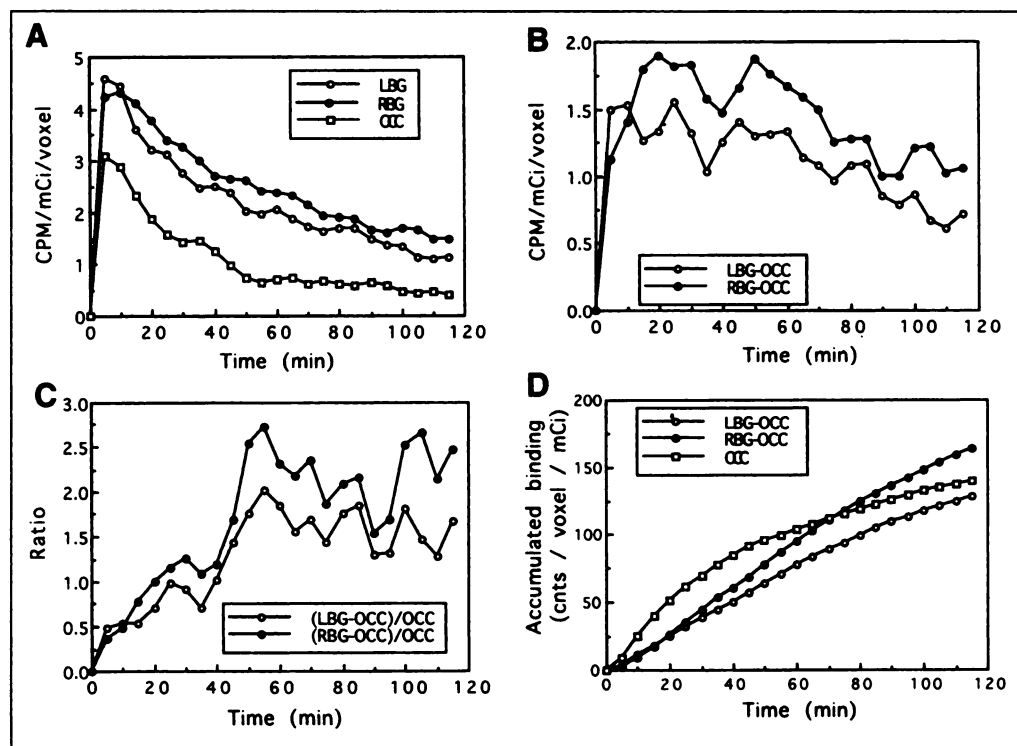


FIGURE 5. IPT time-activity curves for early Parkinson's disease patients (Fig. 3). (A) Tissue curves. (B) Specific binding tissue curves. (C) Empirically defined specific binding ratio (BG - OCC)/OCC. (D) Accumulated specific binding curves.

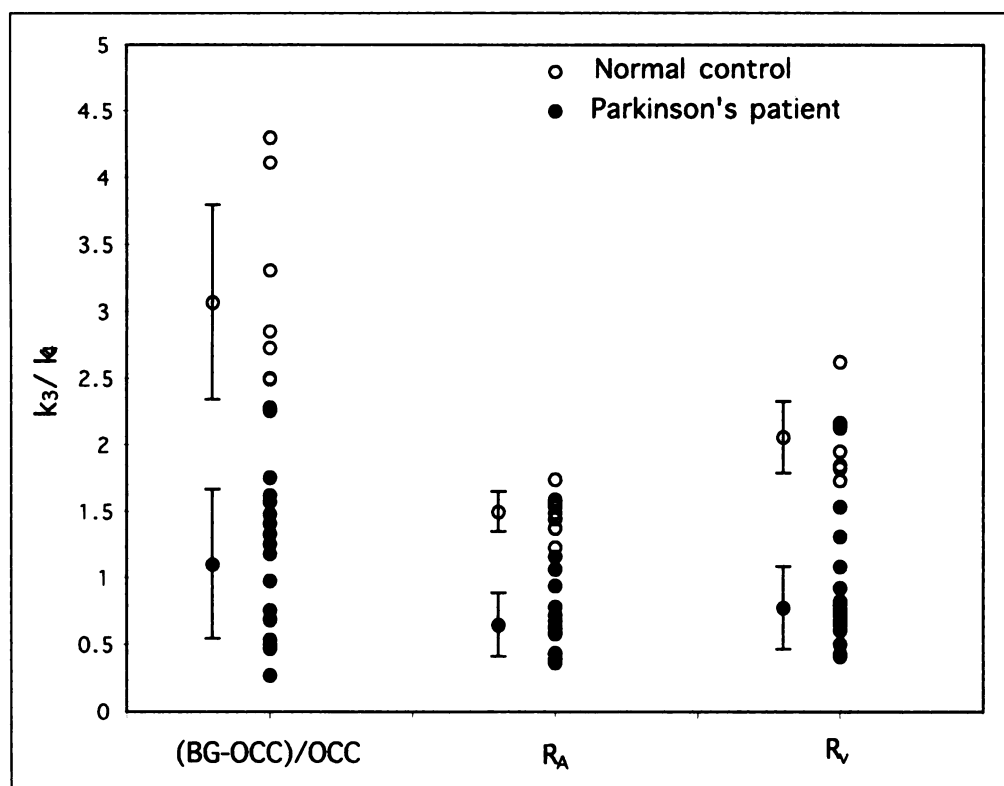


FIGURE 6. (A) Empirically defined ratio (BG - OCC)/OCC at 115 min, graphic method R_V and area ratio method R_A for eight normal controls and 17 early Parkinson's disease patients. ○ = normal controls; ● = Parkinson's disease patients.

in blood flow than changes in transporter concentrations. The ipsilateral (BG - OCC)/OCC, which is the ratio of the side of the body with initial onset of symptoms for unilateral Parkinson's disease, was higher than that of contralateral side, but the ratio of ipsilateral side was much lower than that of normal controls.

Variation of Graphic Method

The variation of graphic method (20,21) was applied to ^{123}I -IPT SPECT dynamic data. The a/a' for normal controls and Parkinson's disease patients were 3.06 ± 0.27 and 1.78 ± 0.31 , respectively. The R_V values were computed by subtracting 1 from a/a' values, and those for normal controls and Parkinson's disease patients were 2.06 ± 0.27 and 0.78 ± 0.31 , respectively (Tables 1 and 2), and p value was 1.91×10^{-8} (Fig. 6). This method uses all of the 2-hr dynamic data and measures k_3/k_4 based on theoretical derivation with equilibrium assumptions (20). The results of this method were used to compare with those of simple method or area ratio method.

Area Ratio Method

The accumulated specific binding for normal controls and Parkinson's disease patients at BG and OCC are shown in Figures 4 and 5. The accumulated binding activities of BG for normal controls have much higher values than those of Parkinson's disease patients, whereas the accumulated bindings of OCC have similar values for both. The mean R_A values for normal controls and Parkinson's disease patients were 1.50 ± 0.15 and 0.65 ± 0.24 , with a p value of 3.46×10^{-10} , respectively, and those for normal controls were clearly separated from Parkinson's disease patients (Fig. 6).

Correlations of (BG - OCC)/OCC at 115 min, R_V and R_A

The relationship between (BG - OCC)/OCC at 115 min or R_A and R_V was examined and shown to be linear, with slopes of 1.54 and 0.66, respectively (Fig. 7). R_A showed a higher correlation ($r = 0.99$) with R_V than did (BG - OCC)/OCC at 115 min with R_V ($r = 0.93$). The mean (BG - OCC)/OCC values for normal controls and Parkinson's disease patients

TABLE 2
(BG - OCC)/OCC, R_A and R_V for Normal Controls

Subject no.	(LBG - OCC)	(RBG - OCC)	(BG - OCC)						
	OCC	OCC	OCC	R_A , LBG	R_A , RBG	R_A	R_V , LBG	R_V , RBG	R_V
NC1	4.43	4.16	4.30	1.80	1.68	1.74	2.75	2.51	2.63
NC2	2.75	2.96	2.85	1.45	1.31	1.38	1.80	1.90	1.85
NC3	2.49	2.52	2.50	1.42	1.48	1.45	1.92	1.98	1.95
NC4	4.09	4.14	4.12	1.58	1.49	1.54	2.18	2.16	2.17
NC5	2.54	2.45	2.50	1.54	1.58	1.56	2.14	2.16	2.15
NC6	3.07	3.55	3.31	1.20	1.27	1.23	1.64	1.83	1.74
NC7	2.83	2.64	2.73	1.59	1.58	1.59	2.13	2.13	2.13
NC8	2.44	2.07	2.26	1.55	1.42	1.49	1.95	1.71	1.83
Mean	3.08	3.06	3.07	1.52	1.48	1.50	2.06	2.05	2.06
s.d.	0.71	0.75	0.73	0.16	0.13	0.15	0.31	0.23	0.27

L = left; R = right; NC = normal control.

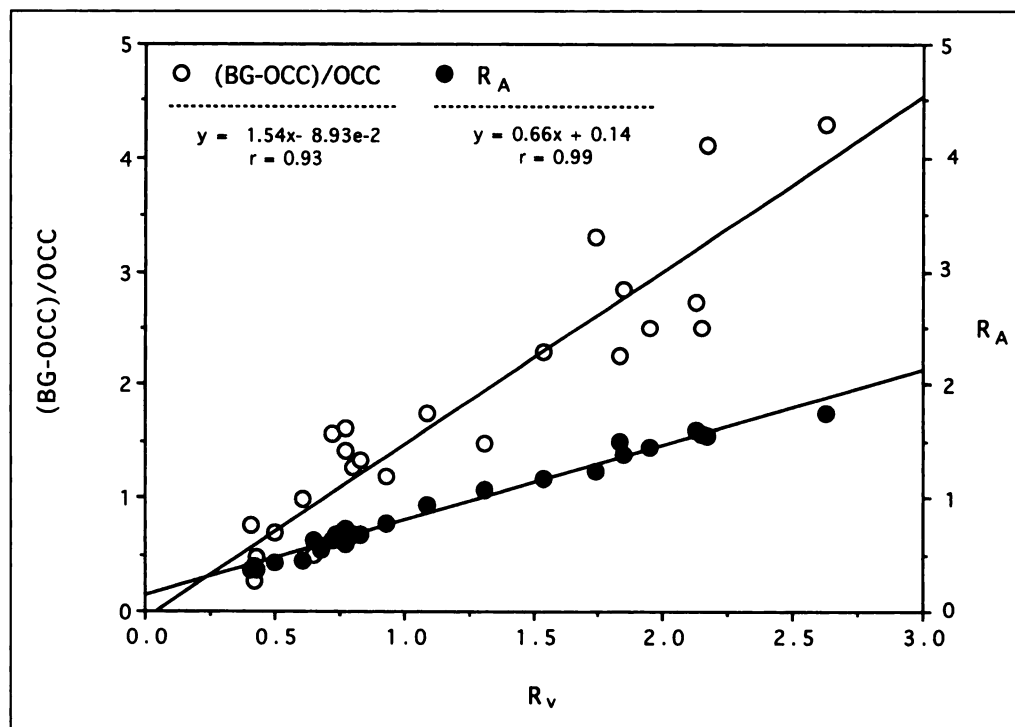


FIGURE 7. Linear relationships between (BG - OCC)/OCC at 115 min and R_A and R_V .

overestimated R_V . This overestimation may be due to a pseudo-equilibrium state that exists at 115 min postinjection. Carson et al. (31) have shown that this causes an overestimation of true receptor density. The mean R_A values for normal controls and Parkinson's disease patients underestimated the mean R_V values. This may be so because time points after 115 min were ignored for the computation of the area under the curve. Ignoring time points after 115 min may cause a greater error in estimation of the total area under the curve (i.e., from 0 to infinity) for BG than that for OCC. In fact, this result would be expected because the washout from BG is slower than that of the OCC, and a more detailed explanation will require the pharmacokinetic computer simulations because it may be too difficult to acquire the dynamic SPECT data for an infinitely longer time. However, all three of the outcome measurements clearly separated Parkinson's disease patients from normal controls (Fig. 6).

DISCUSSION

Dopamine transporter concentrations have been known to decrease in Parkinson's disease patients (14,15) and increase in patients with Tourette's syndrome (11). Several radiopharmaceuticals have recently been developed for imaging dopamine transporters in living human brains. These include ^{11}C -cocaine (7), ^{123}I - β -CIT (10), ^{11}C -WIN 35428 (8) and ^{11}C - β -CIT (9). PET has several advantages in quantitating dopamine transporter concentrations, including better spatial resolution and the capability of attenuation correction, but it is not easily available in clinical environments because it requires cyclotron to produce PET isotopes, such as ^{11}C , ^{18}F , ^{13}N and ^{15}O . Iodine-123- β -CIT with SPECT has widely been used for dopamine transporter imaging, but its washout kinetics are very slow, requiring 24-hr or 48-hr imaging studies (34).

Iodine-123-IPT has recently been developed and applied to image dopamine transporter in baboon and human brains (18,19). The studies showed very high target-to-nontarget ratios, and its washout kinetics are faster than those of ^{123}I - β -CIT, indicating that the full dynamic studies of ^{123}I -IPT could be obtained within 2 hr (19).

These studies support the usefulness of dopamine transporter imaging with ^{123}I -IPT SPECT in differentiating Parkinson's disease patients from normal controls. In this study, we obtained 5-min dynamic SPECT data for 2 hr. These data were then analyzed by three different methods, the empirically defined ratio method of (BG - OCC)/OCC, the theoretically supported graphic method (20,21) and the area ratio method (20,22), to derive the transporter related parameter k_3/k_4 reflecting binding potential. Several assumptions were made for these methods, including that late time-point data may be more sensitive to changes in receptor concentrations than that of blood flow, that distribution volume V_2 is identical in the BG and OCC and that reversibly binding ligands were in a steady state. The pharmacokinetic computer simulation studies, using techniques previously reported (35) for ^{123}I -IPT have shown that the receptor sensitivities at late time point are much higher than blood flow sensitivities (data not shown). The assumption that V_2 is identical in the BG and OCC has widely been used in receptor quantification studies with PET and SPECT (20,32) because it can improve identifiability of the rate constants. Ichise et al. (20) have previously found that there was no effect of regional cerebral blood flow and the peripheral clearance rate in measuring k_3/k_4 using their ^{123}I -IBF-SPECT data.

The BG activities of ^{123}I -IPT in reconstructed images peaked within 10 min postinjection and showed slower washout kinetics for normal controls compared to the Parkinson's disease patients (Figs. 2 and 3), whereas the OCC activities peaked within 5 min postinjection (Figs. 2 and 3). Unlike the BG, the OCC activities for both normal controls and Parkinson's disease patients showed very fast washout kinetics, indicating that the OCC may be a nonspecific site and that there were no differences between normal controls and Parkinson's disease patients. The OCC was used as a nonspecific site in this study. The empiric ratio method of specific binding to nonspecific binding activities (BG - OCC)/OCC has been used to measure receptor parameters, with the assumption that late time point data may be sensitive to changes in receptor concentrations. The average (BG - OCC)/OCC for normal controls was 2.79 times higher than that for Parkinson's disease patients at 115 min.

These differences between normal controls and Parkinson's disease patients may reflect changes in transporter concentrations rather than reflecting changes in blood flow or nonspecific binding activities. However, $(BG - OCC)/OCC$ between normal controls and Parkinson's disease patients were not clearly distinguished for up to 1 hr, indicating that the early time points may be more sensitive to changes in blood flow or nonspecific binding activities than changes in specific binding activities to the transporters. The ipsilateral $(BG - OCC)/OCC$ for unilateral Parkinson's disease was higher than that of contralateral side, but the ratio of ipsilateral side was much lower than that of normal controls, indicating that the transporter concentrations decreased not only in contralateral side but also in ipsilateral side for the unilateral patient. Similar findings were recently reported in patients with hemi-Parkinson's disease investigated with ^{123}I - β -CIT (36). We found a more pronounced reduction of ^{123}I -IPT uptake in the putamen than in the caudate in most Parkinson's disease patients. The average R_V values for normal controls were 2.64 times higher (Tables 1 and 2) than those for Parkinson's disease patients. The theoretically defined R_V values clearly demonstrated that the ^{123}I -IPT reflects changes in transporter concentrations rather than blood flow or nonspecific binding activities. This method uses all of the 2-hr dynamic data and measures k_3/k_4 with equilibrium assumptions. The accumulated bindings of BG for normal controls have much higher values than those of Parkinson's disease patients, whereas the accumulated bindings of OCC have similar values for both groups, indicating that the OCC bindings are nonspecific and may be used as a nonspecific site. The mean value R_A by the area ratio method for normal controls was 2.31 times higher than that for Parkinson's disease patients, and the R_A s for normal controls were clearly separated from Parkinson's disease patients.

The relationship between $(BG - OCC)/OCC$ or R_A and R_V was linear, with slopes of 1.54 and 0.66, respectively (Fig. 7). R_A showed a higher correlation ($r = 0.99$) with R_V than did $(BG - OCC)/OCC$ at 115 min ($r = 0.93$). R_A underestimated R_V , and $(BG - OCC)/OCC$ overestimated R_V . $(BG - OCC)/OCC$, R_A and R_V all clearly separated Parkinson's disease patients from normal controls. Several previous studies have shown that dopamine transporter binding as measured by ^{123}I - β -CIT and SPECT is inversely correlated with age (37,38). Recently, ^{123}I -IPT SPECT studies suggested that the effects of aging may be nonlinear so that the decrease of transporter density with age, as measured by striatal ^{123}I -IPT uptake, is less marked in persons older than 40 yr than it is in young patients (38,39). The differences between normal controls and Parkinson's disease patients in $(BG - OCC)/OCC$, R_V and R_A that were shown in this study could be marginally affected by aging because both normal controls and Parkinson's disease patients were older than 40 yr.

CONCLUSION

Iodine-123-IPT SPECT dynamic data provided good BG-to-OCC ratios with relatively fast washout kinetics, indicating reversible binding. These conditions are necessary to measure changes in dopamine transporter concentrations (32). The $(BG - OCC)/OCC$, R_V and R_A for PP were clearly separated from those of normal controls and may be very useful outcome measures for clinical diagnosis. The simplest $(BG - OCC)/OCC$ ratio, requiring a single late time point, could be useful in clinical situations, although it should be noted that this measurement, under pseudoequilibrium conditions, may overestimate the number of transporters in a nonlinear manner, whereas R_V is preferred when the dynamic data are available. However,

the findings suggest that ^{123}I -IPT may be a very useful tracer for early diagnosis of Parkinson's disease and studying dopamine reuptake sites.

ACKNOWLEDGMENTS

This work was supported by Grants AIFLC95-127 and AIFLC 96-127 from the Asian Institute for Life Sciences and, in part, by Grant CRAM1-1 from the Center for Radioisotope Applied Materials.

REFERENCES

- Johanson CE, Fischman M. The pharmacology of cocaine related to its abuse. *Pharmacol Rev* 1989;41:3-52.
- Rudnick G, Clark J. From synapse to vesicle: the reuptake and storage of biogenic amine neurotransmitters. *Biochim Biophys Acta* 1993;1144:249-263.
- Ritz M, Lamb R, Goldberg S, Kuhar M. Cocaine receptors on dopamine transporters are related to self-administration of cocaine. *Science* 1987;237:1219-1223.
- Innis R, Baldwin R, Sybirska, et al. Single photon emission computed tomography imaging of monoamine reuptake sites in primate brain with [^{123}I]- β -CIT. *Eur J Pharmacol* 1991;200:369-370.
- Kapur S, Mann J. Role of the dopamine system in depression. *Biol Psychiatry* 1992;32:1-7.
- Shaya E, Scheffel U, Dannals R, et al. In vivo imaging of dopamine reuptake sites in the primate brain using single-photon emission computed tomography (SPECT) and iodine-123 labeled RTI-55. *Synapse* 1992;10:169-172.
- Scheffel U, Dannals RF, Wong DF, Yokoi F, Carrol FI, Kuhar MJ. Dopamine transporter imaging with novel, selective cocaine analogs. *Neuroreport* 1992;3:969-972.
- Wong DF, Yung B, Dannals RF, et al. In vivo imaging of baboon and human dopamine transporters by positron emission tomography using [^{11}C]WIN 35,428. *Synapse* 1993;15:130-142.
- Muller L, Halldin C, Farde L, et al. Carbon-11- β -CIT, a cocaine analog-preparation, autoradiography and preliminary PET investigations. *Nucl Med Biol* 1993;20:249-255.
- Laruelle M, Baldwin R, Malison R, et al. SPECT imaging of dopamine and serotonin transporters with [^{123}I] β -CIT: pharmacological characterization of brain uptake in nonhuman primates. *Synapse* 1993;13:295-309.
- Malison RT, McDougle CJ, van Dyck CH, et al. [^{123}I] β -CIT SPECT imaging of striatal dopamine transporter binding in Tourette's disorder. *Am J Psychiatry* 1995;152:1359-1361.
- Fowler J, Volkow N, Wolf A, et al. Mapping cocaine binding sites in human and baboon brain in vivo. *Synapse* 1989;4:371-377.
- Yu D, Gately S, Wolf A, et al. Synthesis of carbon-11-labeled iodinated cocaine derivatives and their distribution in baboon brain measured using positron emission tomography. *J Med Chem* 1992;35:2178-2183.
- Frost JJ, Rosier A, Reich S, et al. Positron emission tomographic imaging of the dopamine transporter with [^{11}C]WIN 35,428 reveals marked declines in mild Parkinson's disease. *Ann Neurol* 1993;34:423-431.
- Innis R, Seibyl J, Scanley B, et al. Single-photon emission computed tomographic imaging demonstrates loss of striatal dopamine transporters in Parkinson's disease. *Proc Natl Acad Sci USA* 1993;90:11965-11969.
- Goodman M, Kung M, Kabalka G, Kung H, Switzer R. Synthesis and characterization of radioiodinated N-(3-iodopropene-2-yl)-2b-carbomethoxy-3b-(4-chlorophenyl) tropanes: potential dopamine reuptake site imaging agents. *J Med Chem* 1994;37:1535-1542.
- Kung MP, Essman WD, Frederick D, et al. IPT: a novel iodinated ligand for the CNS dopamine transporter. *Synapse* 1995;320:316-324.
- Malison RT, Vessotskie JM, Kung MP, et al. Striatal dopamine transporter imaging in nonhuman primates with iodine-123-IPT SPECT. *J Nucl Med* 1995;36:2290-2297.
- Mozley PD, Stubbs JB, Kim H-J, et al. Dosimetry of an iodine-123-labeled tropane to image dopamine transporters. *J Nucl Med* 1996;37:151-159.
- Ichise M, Ballinger JR, Golan H, et al. Noninvasive quantification of dopamine D2 receptors with iodine-123-IBF SPECT. *J Nucl Med* 1996;37:513-520.
- Logan J, Fowler JS, Volkow ND, et al. Graphical analysis of reversible radioligand binding from time-activity measurements applied to [^{11}C -methyl]-(-)-cocaine PET studies in human subjects. *J Cereb Blood Flow Metab* 1990;10:740-747.
- Lassen NA. Neuroreceptor quantitation in vivo by the steady-state principle using constant infusion or bolus injection of radioactive tracers. *J Cereb Blood Flow Metab* 1992;12:709-716.
- Stern MD. Rating the parkinsonian patient. In: Stern MB, Hurtig HI, eds. *The comprehensive management of Parkinson's disease*. New York: PMA Publishing Corp., 1988:3-50.
- Hoehn MM, Yahr MD. Parkinsonism: onset, progression and mortality. *Neurology* 1967;17:427-442.
- Zea-Ponce Y, Baldwin RM, Laruelle M, Wang S, Neumeyer JL, Innis RB. Simplified multidose preparation of iodine-123- β -CIT: a marker for dopamine transporters. *J Nucl Med* 1995;36:525-529.
- Myers AM, Meegalla SK, Kung M-P, Kung HF. Metabolic analysis of I-123 IPT: a new dopamine reuptake site imaging agent [Abstract]. *J Nucl Med* 1995;36(suppl):124.
- Chang LT. A method for attenuation correction in radionuclide computed tomography. *IEEE Trans Nucl Sci* 1978;25:638-643.
- Muller-Gartner HW, Wilson AA, Dannals RF, Wagner HN Jr, Frost JJ. Imaging muscarinic cholinergic receptors in human brain in vivo with SPECT, [^{123}I]-4-iododexetimide and [^{123}I]-4-iodolevetimide. *J Cereb Blood Flow Metab* 1992;12:562-570.

29. Farde L, Hall H, Ehrn E, Sedvall G. Quantitative analysis of D2 dopamine receptor binding in the living human brain by PET. *Science* 1986;231:258–261.
30. Frost JJ, Douglass KH, Mayberg HS, et al. Multicompartmental analysis of [¹¹C]-[carfentanil binding to opiate receptors in humans measured by positron emission tomography. *J Cereb Blood Flow Metab* 1989;9:398–409.
31. Carson RE, Channing MA, Blasberg RG, et al. Comparison of bolus and infusion methods for receptor quantitation: application to [¹⁸F]-cyclofexy and positron emission tomography. *J Cereb Blood Flow Metab* 1993;13:24–42.
32. Laruelle M, van Dyck C, Abi-Dargham A, et al. Compartmental modeling of iodine-123-iodobenzofuran binding to dopamine D2 receptors in healthy subjects. *J Nucl Med* 1994;35:743–754.
33. Nadeau SE, Couch MW, Devane L, Shukla SS. Regional analysis of D2 dopamine receptors in Parkinson's disease using SPECT and iodine-123-iodobenzamide. *J Nucl Med* 1995;36:384–393.
34. Kim SE, Lee WY, Chi DY, et al. SPECT imaging of dopamine transporter with [¹²³I]-β-CIT: a potential clinical tool in Parkinson's disease. *Korean J Nucl Med* 1996;30:19–34.
35. Kim HJ, Zeeberg BR, Reba RC. Theoretical investigation of the estimation of relative regional neuroreceptor concentration from a single SPECT or PET image. *IEEE Trans Med Imaging* 1990;9:247–261.
36. Marek KL, Seibyl JP, Zoghbi SS, et al. [¹²³I]-β-CIT SPECT imaging demonstrates bilateral loss of dopamine transporters in hemi-Parkinson's disease. *Neurology* 1996;46:231–237.
37. van Dyck CH, Seibyl JP, Malison RT, et al. Age-related decline in striatal dopamine transporter binding with iodine-123-β-CIT SPECT. *J Nucl Med* 1995;36:1175–1181.
38. Mozley PD, Kim H-J, Gur RC, et al. Iodine-123-IPT SPECT imaging of CNS dopamine transporters: nonlinear effects of normal aging on striatal uptake values. *J Nucl Med* 1996;37:1965–1970.
39. Tatsch K, Schwarz J, Mozley PD, et al. Relationship between clinical features of Parkinson's disease and presynaptic dopamine transporter binding assessed with [¹²³I]-IPT and SPECT. *Eur J Nucl Med* 1997: in press.

Iodine-123-Epidepride-SPECT: Studies in Parkinson's Disease, Multiple System Atrophy and Huntington's Disease

Walter Pirker, Susanne Asenbaum, Sylvia Wenger, Johannes Kornhuber, Peter Angelberger, Lüder Deecke, Ivo Podreka and Thomas Brücke

University Clinics for Neurology and Nuclear Medicine, Vienna, Austria; Department of Psychiatry, University of Göttingen, Göttingen, Germany; and Forschungszentrum Seibersdorf, Seibersdorf, Austria

Epidepride is a benzamide derivative with very high affinity for D2 receptors, which, in its [¹²³I]-labeled form, can be used for SPECT. The aim of this study was to evaluate the usefulness and accuracy of [¹²³I]epidepride-SPECT for the differential diagnosis of movement disorders. **Methods:** SPECT imaging with a triple-headed scintillation camera was performed in 9 patients with Parkinson's disease, 9 patients with probable multiple system atrophy (MSA), 1 patient with progressive supranuclear palsy, 16 patients with Huntington's disease (HD) and 14 controls, 3 hr after the intravenous injection of 3.7 ± 1.3 mCi of [¹²³I]epidepride. The striatum-to-cerebellum ratio – 1, reflecting the specific-to-nondisplaceable binding ratio, was used as a semiquantitative measure of D2 receptor binding. **Results:** Kinetic studies showed peak striatal uptake about 3 hr postinjection and a slow decline thereafter. The striatum-to-cerebellum ratio – 1 was significantly reduced in MSA (11.8 ± 3.9 , compared to controls, 19.0 ± 6.3 ; $p < 0.01$) and in patients with HD (8.8 ± 3.2 ; $p < 0.00005$) but normal in Parkinson's disease (15.8 ± 3.6 ; not significant). A high interindividual variation of specific striatal epidepride binding (striatum – cerebellum; cpm/mCi \times kg) was found in controls and in all patient groups. The interindividual variation of striatum-to-cerebellum ratios was lower but still considerable. In half of the MSA patients, the specific-to-nondisplaceable binding ratio fell within the range of controls. The use of various cortical reference regions did not improve discrimination between MSA and controls or Parkinson's disease patients, respectively. The discrimination of HD patients from controls was better, with overlap in only two cases. In one HD patient, calculation of the striatum-to-cerebellum ratio was almost impossible due to extremely low nonspecific binding. Possible explanations for the large variation of the ratios, resulting in an overlap between controls and different patient groups, are very low counting rates in the reference region and the fact that a transient binding equilibrium may not be achieved after bolus injection of epidepride. **Conclusion:** Epidepride appears to be a useful SPECT ligand for studying dopamine D2 receptors. However,

its markedly higher specific-to-nondisplaceable binding ratio in comparison to those of iodobenzamide or other D2 ligands did not result in a better discrimination between different basal ganglia disorders. The calculation of plasma input curves and volumes of distribution might improve the accuracy of [¹²³I]epidepride-SPECT.

Key Words: dopamine; D2 receptors; epidepride; SPECT; basal ganglia disorders

J Nucl Med 1997; 38:1711–1717

Since the early 1980s, in vivo imaging of the postsynaptic side and, more recently, of the presynaptic side of the nigrostriatal dopaminergic system has contributed significantly to our understanding of a variety of neuropsychiatric disorders. Dopamine D2 receptors have been studied with PET using butyrophenone derivatives such as [¹¹C]N-methylspiperone (1) and substituted benzamides like [¹¹C]raclopride (2). The first D2 receptor imaging study with SPECT was performed using [⁷⁷Br]spiperone (3). Because of their almost irreversible binding to D2 receptors, imaging studies with spiperone derivatives cannot be performed at equilibrium, and receptor binding can only be determined by performing dynamic studies and complicated mathematical calculations (4). The introduction of the benzamide [¹²³I]iodobenzamide (IBZM), which allowed imaging under pseudoequilibrium conditions and semiquantification with a simple ratio method using SPECT, led to a broader clinical application of D2 receptor imaging (5–7). Iodine-123-IBZM-SPECT was shown to be an effective tool for the differential diagnosis of Parkinson's disease and parkinsonism related to other neurodegenerative disorders, such as multiple system atrophy (MSA) and progressive supranuclear palsy (8–12) and drug-induced parkinsonism (7,13–15). However, IBZM has certain disadvantages as a SPECT ligand for D2 receptors; with a K_D of ~ 0.4 nM (16,17), the affinity for the D2 receptor is relatively moderate. Iodobenzamide is a highly

Received Nov. 7, 1996; revision accepted Mar. 11, 1997.

For correspondence or reprints contact: Walter Pirker, MD, Neurological University Clinic, Währinger Gürtel 18-20, A-1090 Vienna, Austria.